ACCSCIENCE PUBLISHING

Green Technology & Innovation

ARTICLE

Lime-plaster enhanced with phase-change materials: An experimental monitoring analysis

Eleonora Baccega* and **Michele Bottarelli**

Department of Architecture, University of Ferrara, Ferrara, Italy

Abstract

The building sector strongly affects the energy required for development, especially for heating and cooling processes. The need to reduce the energy demand and environmental impact must contend with the ever-increasing energy demand within buildings and obsolete building stock. The design and construction of new energy-efficient buildings are inadequate to address the issue, which can only be effectively tackled by improving existing buildings. Given that a significant number of these existing buildings are individually protected or located within protected contexts, interventions can be challenging due to several limitations that reduce the number of possible strategies that can be adopted. Therefore, strategies for the energy refurbishment of historical buildings – particularly those integrated within the building envelope – are crucial to achieving the ambitious aim of reducing the environmental impact of the building sector. The effectiveness of phase change materials (PCMs) was investigated when integrated within lime-based plasters for application on the outermost layer of walls. Experimental tests under real outdoor conditions were carried out initially to estimate whether, and to what extent, the addition of PCMs affected the thermal behavior of walls and the building's energy demand for cooling. Plasters with different PCMs were developed and arranged in a customized setup at the TekneHub Laboratory, University of Ferrara, and subsequently tested over several months. The results demonstrated good performance in attenuating daily temperature fluctuations and reducing energy consumption.

Keywords: Phase-change materials; Lime plaster; Building energy refurbishment; Historical buildings

***Corresponding author:**
Eleonora Baccega
(eleonora.baccega@unife.it)

Citation: Baccega E, Bottarelli M. Lime-plaster enhanced with phase-change materials: An experimental monitoring analysis. *Green Technol Innov.* 2025;1(1):8108. doi: 10.36922/gti.8108

Received: December 21, 2024

Revised: April 3, 2025

Accepted: April 7, 2025

Published online: May 8, 2025

1. Introduction

The building and construction sector is the largest energy-consuming sector,[1] accounting for almost one-third of the global energy consumption and almost 40% of total related CO_2 emissions.[2] Residential buildings are the primary contributors, with an energy demand about three times higher than non-residential buildings.[3] The urban heat island effect, rising living standards, and the decreasing cost of cooling equipment further exacerbate the energy demand for heating, ventilation, and air-conditioning systems, especially during the summer season.[4,5] In addition, a significant portion of the building stock consists of old and obsolete buildings with energy performance that do not meet the present standards. For example, in Italy, about 70% of the buildings were built before the introduction of the first law that established the limits for energy

consumption, enacted in 1976.[6,7] At the same time, the construction rate of new buildings is only about 1%/year.[8] Based on these assumptions, interventions on existing buildings aimed at their energy refurbishment seem to be of utmost importance. However, such interventions are not easily feasible in the case of particular buildings protected by regulatory restrictions due to esthetic qualities, cultural relevance, or located within sensitive areas, such as historical city centers. In these contexts, the so-called passive design strategies emerge as a viable solution for simultaneously improving building performance and indoor comfort without placing additional stress on energy demand.[9] Song *et al.*[10] categorized conventional passive cooling strategies into three main groups: Solar and heat control, heat removal, and heat exchange reduction. Solar and heat control strategies usually consist of shades and are aimed at limiting heat transmission into buildings. Conversely, heat removal strategies are aimed at removing heat in buildings and can be achieved by means of natural ventilation, among others. Finally, heat exchange reduction mainly consists of intervention on the building envelope that can be achieved with or without thermal mass. Strategies with thermal mass include, for instance, the application of phase change materials (PCMs), through which the building envelope's thermal inertia is increased and the indoor thermal comfort is improved by reducing indoor temperature fluctuations.[11,12] The present study evaluated the addition of granular PCMs into lime-based plaster as a potential strategy for energy refurbishment of historical and protected buildings. The study involved preliminary experimental tests performed at a lab scale at the TekneHub Laboratory, University of Ferrara, aimed at the thermophysical characterization of different plasters enhanced with PCM, as previously reported.[13,14] The research was subsequently scaled up. Plaster samples with different concentrations of PCM were prepared and then tested under real outdoor conditions for several weeks, with the results presented here representing a selection of some of the data acquired. These data were then used to validate a numerical model, enabling further investigations in which different boundary conditions, wall configurations, and PCM properties could be defined.

2. Methods

The tests carried out at a lab scale aimed to preliminarily investigate the effect of PCM when mixed into plasters. The promising results obtained led to the next phase of research, which involved monitoring the materials under real outdoor conditions. This part of the research was conducted in collaboration with Fassa Bortolo,[15] an Italian industry leader in the production of mortars, pre-mixed plasters, paints, and thermal insulation. A setup was designed and constructed to simultaneously monitor up to four wall samples. The installation took place in an existing mock-up building at the TekneHub Laboratory, University of Ferrara, which was built in 2016 as part of the European project LIFE Climate Change Adaptation – HEROTILE.[16] The mock-up building has a rectangular 10 × 8 m plan and is made of five adjacent independent test rooms and two guard rooms, one on each side, ensuring identical boundary conditions in each test room. For this research, one of these test rooms was used, and part of the southern façade was removed to allow the installation of the wooden setup, as represented in Figure 1.

2.1. Experimental setup

The aforementioned setup has an aluminum structure clad with oriented strand board panels and was intended for simultaneous tests of up to four wall samples. The setup was about 90 × 90 × 50 cm, while each available slot, where the wall samples were positioned, was 38 × 38 × 50 cm.

Each wall sample consisted of a 6 cm brick layer coated with 3 cm plaster on both exterior and interior sides. To ensure maximum flexibility for the system, the wall samples were made by coupling two identical parts, each consisting of a 3 cm masonry tile covered by 3 cm of plaster. These parts were then held together with wooden frames and metal profiles (Figure 2). The wall samples were 30 × 30 cm and had a 4 cm insulation frame all around to limit heat transfer at the edges, thereby ensuring one-dimensional heat transfer through the wall sample. Images of the setup and the installation of the plaster samples are reported in Figure 3.

2.2. Monitoring system

A monitoring system was also implemented to collect data on temperatures and heat fluxes for each configuration. T-type thermocouples, with an accuracy of ± 0.5°C, were installed on the exterior and interior plaster surfaces, as well as inside the mock-up room, to monitor air temperature. Heat flux meters, with an accuracy of ± 5%, and an integrated temperature sensor, with an accuracy of ± 2%,[17] were positioned between the two brick layers,

Figure 1. South façade of the mock-up with the wooden setup installed

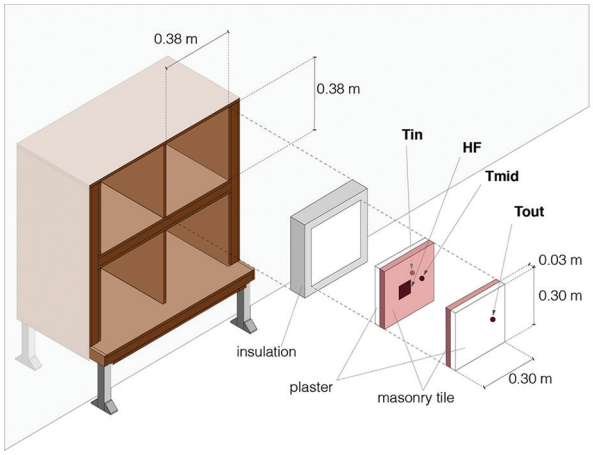

Figure 2. Schematic representation of the setup: Material and sensor position
Abbreviations: T: Temperature; HF: Heat flux.

Figure 3. Plaster sample installation and view of the complete installation

corresponding to the middle of each wall sample. These sensors were connected to a datalogger, a DataTaker DT85 series 3 (Italy),[18] which acquired data with a timestep of 1 min. Boundary conditions, including air temperature, solar radiation, wind speed, and wind direction, were monitored through a weather station,[19] previously installed near the mock-up. An additional pyranometer[20] was vertically installed near the mock-up to acquire data on vertical hemispherical irradiance, which was later used to validate the numerical model implemented.

2.3. Constructed samples

During monitoring, different plaster samples and wall configurations were tested. For this research, two different granular PCMs were used; the first PCM AS28 (Smart Advanced Systems GmbH, Germany)[21] had a phase change temperature of approximately 28°C and an active PCM content of 70 – 80%; the other PCM TK27 (TITK, Germany)[22] had a phase change temperature of approximately 27°C and an active PCM content of approximately 75%. Monitoring began with testing four different plaster samples: A reference sample (used as the benchmark) and three samples containing granules of PCMs. More specifically, two of these samples were developed by adding 10% and 30% by mass of AS28; the third sample was developed by adding 10% by mass of TK27. The comparison between samples containing different quantities of the same PCM was carried out to evaluate how the amount of PCM influences its effect. Meanwhile, the comparison between samples containing different PCMs aimed to evaluate how the thermal properties of various PCMs impact performance. After several weeks of monitoring, degradation was observed in the plaster containing 30% PCM, likely due to an excessive amount of PCM. Consequently, an additional plaster was created, enhanced with 20% by mass of AS28, which was later added and tested. The thermophysical properties of the reference and enhanced plasters were estimated during the lab-scale tests,[13,14] and the values are summarized in Table 1, along with the adopted nomenclature.

Except for the 20AS28 sample, which was produced in the lab to compensate for the unexpected degradation of the 30AS28 sample, all plaster samples were prepared by Fassa Bortolo at their facility. No significant issues were encountered in the preparation at this scale. The only precaution taken was to add the PCM granules to the dry premix, with water added only after the dry aggregates were thoroughly mixed.

2.4. Monitoring

Monitoring was conducted from April to August, 2022. Different monitoring periods were defined based on the configurations tested or the boundary conditions. The two periods are described below.

Period I began at the start of the monitoring activity and ended on June 15, 2022. During this phase, one of the four wall samples – referred to as the Reference – featured the reference plaster on both the inner and outer surfaces. The remaining three wall samples had the reference plaster on the inner surface and one of the plasters containing PCM on the outer surface, namely, 10TK27, 10AS28, and 30AS28.

Period II began on August 4, 2022, and lasted until August 31, 2022. In this configuration, the wall sample treated with 10TK27 was modified to include the newly prepared plaster (20AS28) on the outer surface. The wall configurations tested are summarized in Figure 4.

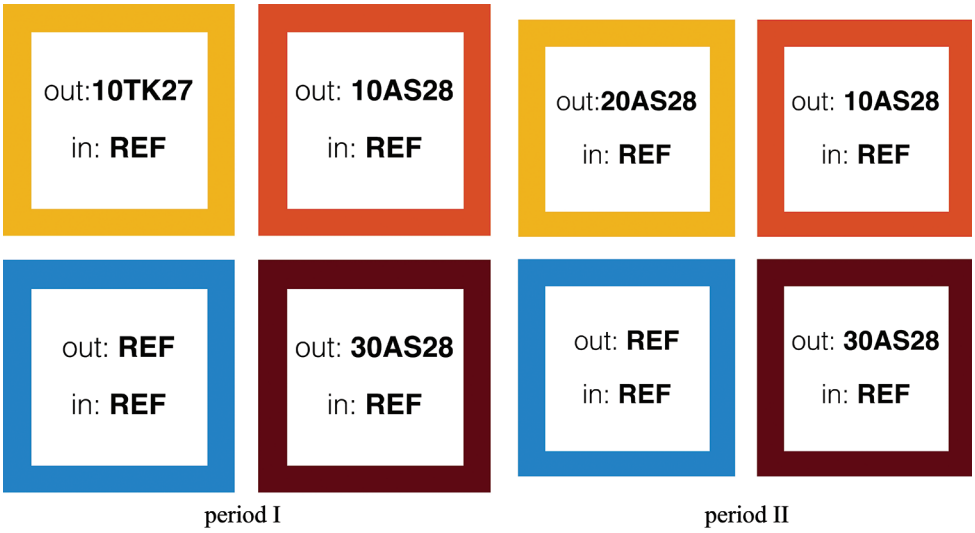

Figure 4. Configurations were tested in the two periods

Table 1. Estimated thermophysical properties of the plasters tested

Plaster	PCM type	PCM mass ratio (%)	p (kg/m^3)	λ (W/[m·K])	c_p (kJ/[kg·K])	L_h (kJ/kg)
Reference	-	-	1646	0.31	0.9	-
10AS28	AS28	10	1522	0.28	1.1	9.2
20AS28	AS28	20	1402	0.26	1.2	18.4
30AS28	AS28	30	1321	0.24	1.3	27.6
10TK27	TK27	10	1365	0.24	1.1	11.9

Abbreviations: PCM: Phase change material; c_p: Specific heat; L_h: latent heat; ρ: Density; λ: Thermal conductivity.

3. Results and discussion

3.1. Period I

The boundary conditions that characterized period I are reported in Table 2. The average temperature was 25.1°C during the day and 18.3°C during the night, while the maximum and minimum temperatures achieved were 33.9 and 7.4°C, respectively. The maximum solar irradiance was 1068 W/m^2, with an average of 435 W/m^2 during the whole day and 636 W/m^2 in the interval 12:00 – 15:00. The interval May 11 – 16 was chosen as the most representative period, with corresponding boundary conditions reported in Figure 5. During this period, the lowest temperatures were between 15°C and 18°C, while the highest temperature was approximately 30°C. Similarly, solar irradiance reached peak values of 850 W/m^2, with cloudy skies only on May 14 and 15. Moreover, no rainfall was observed during this period.

Figure 6 depicts the temperatures on the outer plaster surfaces. The differences among the wall samples were limited to the hottest hours of the day. During the period between late afternoon and early morning, temperature differences were lower than 0.5°C, which is the sensors' accuracy limit. Both 10AS28 and 10TK27 reached lower maximum values than the Reference, with differences of 1 – 2°C. For 30AS28, the maximum values are higher than the reference, with differences of up to 2 – 3°C. This observation could be due to issues in the sensor's positioning from plaster deterioration, as represented in Figure 7. Plaster deterioration can be caused by the volumetric expansion of the PCM during phase change, which is exacerbated by the high mass ratio of the PCM.

Table 2. Average boundary conditions in period I

Condition	Day	Night	Interval
Average outdoor temperature (°C)	25.1	18.3	26.4
Maximum outdoor temperature (°C)	33.9	28.6	32.9
Minimum outdoor temperature (°C)	12.3	7.4	13.6
Average indoor temperature (°C)	23.2	20.5	24.0
Average solar irradiance (W/m^2)	435	35	636
Maximum solar irradiance (W/m^2)	1068	479	1068
Solar gain (kWh/[m^2 day])	5.22	0.42	2.54

Note: The time intervals are defined as: (i) Day: 9:00 – 20:00; (ii) Night: 20:00 – 9:00; and (iii) Interval: 12:00 – 15:00.

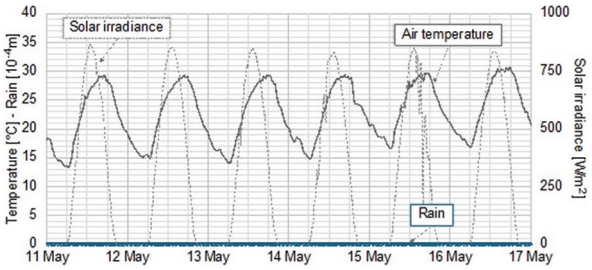

Figure 5. Boundary conditions in the selected interval of period I

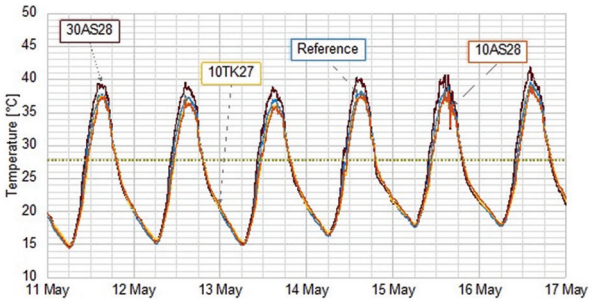

Figure 6. Outer surface temperatures (Tout) in period I

Figure 7. Deterioration of 30AS28

As depicted in Figure 8, temperatures on the inner plaster surfaces for Reference, 10AS28, and 10TK27 are almost identical, with non-significant differences that are below the sensors' accuracy. A relevant difference is observed in the case of 30AS28, whose temperature was 1°C higher during the night and about 1.5°C lower during the day, suggesting that the temperature on the inner surface was overall more stable, with lower fluctuations. In all three samples (Reference, 10AS28, and 10TK27), the temperature fluctuated between 17°C and 26°C; conversely, the temperature of 30AS28 fluctuated between 18°C and 25°C. The greatest temperature differences are observed

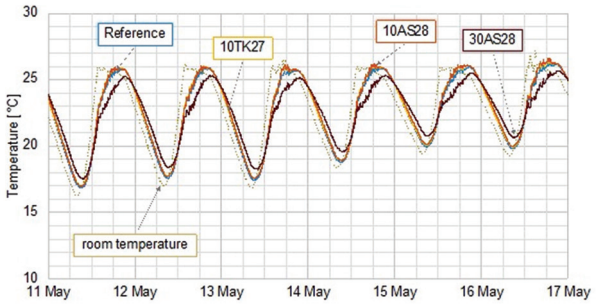

Figure 8. Inner surface temperatures (Tin) in period I

in the middle of the wall samples, corresponding to T_{mid}, depicted in Figure 9. It can be observed that temperatures in Reference, 10AS28, and 10TK27 have the same trend and limited differences; in 30AS28, the trend is relatively different, with 2 – 3°C higher minimum values and up to 4°C lower maximum values. From the temperature curves, it is also possible to identify the phase change, which is highlighted in the graph (Figure 9). The change in slope – a slowdown in the temperature change during both heating and cooling – corresponds to the melting or the solidification of the PCM, which absorbs and releases a significant amount of energy while maintaining an almost constant temperature during its phase change. To better compare the wall samples, differences between the temperatures in the middle of the Reference and those of each wall containing PCM are depicted in Figure 10. In both 10AS28 and 10TK27, the maximum temperatures reached were 1°C lower than the reference, while the minimum values were up to 1°C higher. Nevertheless, although the two enhanced wall samples displayed nearly identical temperature differences, these did not occur simultaneously. The differences are observed during the phase change of each PCM, which occurs at slightly different temperatures. In 10TK27, the phase change occurs before that of 10AS28 during the day; hence, the PCM starts to melt at a lower temperature (which corresponds to what was observed from the differential scanning calorimetry). In addition, PCM solidifies at a lower temperature during the night as phase change happens later than that of 10AS28. These differences are more clearly observed in the heat flux data (Figure 11). Outward and inward heat fluxes in the reference wall sample are greater than the other wall samples containing PCM. In 10AS28 and 10TK27, the minimum and maximum values reached are similar and lower in absolute terms than the Reference, respectively, but the trends are quite different. In the case of 10TK27, relative to the Reference, the curve appears slightly flattened, but the phase change is not visible, neither during melting nor solidification. On the contrary, for 10AS28, noticeable slope changes can be observed, allowing the identification

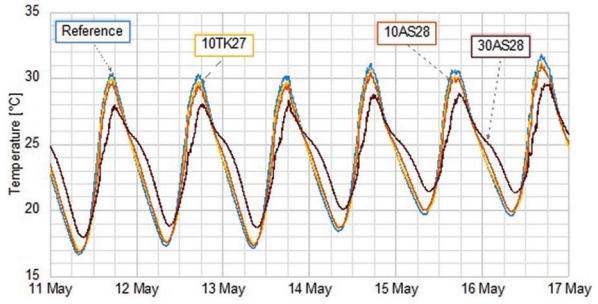

Figure 9. Temperatures in the middle (Tmid) of the wall samples in period I

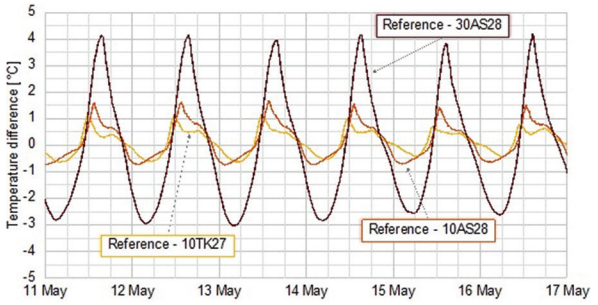

Figure 10. Temperature differences in the middle of the wall samples compared to the reference in period I

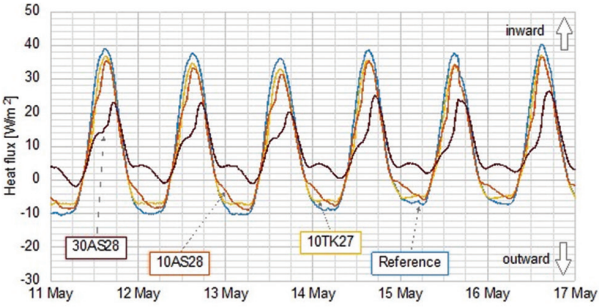

Figure 11. Heat fluxes in the middle of the wall samples in period I

of the phase change occurring both during the day and at night. For a better understanding of the differences, the heat flux data comparing the reference to 10AS28 and 10TK27 are depicted in Figure 12A and B, respectively. Moreover, the areas corresponding to a reduction of the inward and outward heat fluxes in the case of the PCM-enhanced samples are highlighted. From this comparison, the difference between the curves of 10AS28 and 10TK27 is clearly visible. Finally, there was a consistent reduction in heat flux for 30AS28 both during the day and at night, with phase change observed from changes in the slope. Notably, compared to the other wall samples, the heat flux is mostly inward during the night. This is due to the phase change of the PCM that, during solidification, releases the absorbed energy, part of which goes inward through the envelope. Nonetheless, the additional inward energy does not affect the energy demand for cooling, as this phenomenon happens during the night when the indoor temperature is much lower than the set point temperature. Figure 13 presents the inward energy transfer through each of the wall samples during the selected interval with the fan coil turned on. The energy through the reference is the highest (1.32 kWh/m^2), followed by 10TK27 (1.18 kWh/m^2), 10AS28 (1.12 kWh/m^2), and 30AS28 (0.84 kWh/m^2). Hence, the use of PCM led to a reduction in incoming energy of 10.6% for 10TK27, 15.2% for 10AS28, and 36.4% for 30AS28.

Some assumptions were made for the data acquired in the period I. In Figure 14, the differences between the heat flux through the reference and each of the wall samples containing PCM are depicted, along with temperatures monitored on the outer plaster surface and the middle of the wall sample. A recurring pattern, which is highlighted in Figure 14, can be observed each day the temperature on the outer surface reached at least 35°C during the day and 18 – 20°C during the night, while the temperature in the middle of the wall sample fluctuated between 28°C and 30°C during the day and 20 – 22°C during the night. In all the other days in which the maximum outdoor air temperature and outer surface temperature reached lower values, the differences between the heat fluxes are more limited due to incomplete PCM phase change. For 30AS28, the incoming heat flux is up to 25 W/m^2 lower than the reference during the day and up to 15 W/m^2 lower than the reference during the night. The heat flux differences for 10TK27 and 10AS28 are relatively similar (i.e., 10 W/m^2 lower during the day and up to 8 W/m^2 lower during the night) but with different trends. In the case of 10AS28, for each day, two peaks are visible; one corresponding to the reduction of the incoming heat flux due to PCM melting and the other one during the night due to PCM solidification. In contrast, for 10TK27, only one peak is visible during the day, while during the night, the difference appears to be spread over a longer period. The different behavior of these – despite containing the same amount of PCM – can be attributed to the different PCM properties, more specifically to the different temperature intervals over which the phase change occurs. The phase change of TK27 occurs over a much wider temperature interval than AS28, and this leads to more limited differences but distributed over a longer period. Notably, the visible differences between melting and solidification are influenced by the PCM properties. It is common for PCMs to behave differently during melting or solidification – a phenomenon known as hysteresis – which was observed during lab-scale tests.[14] Based on all

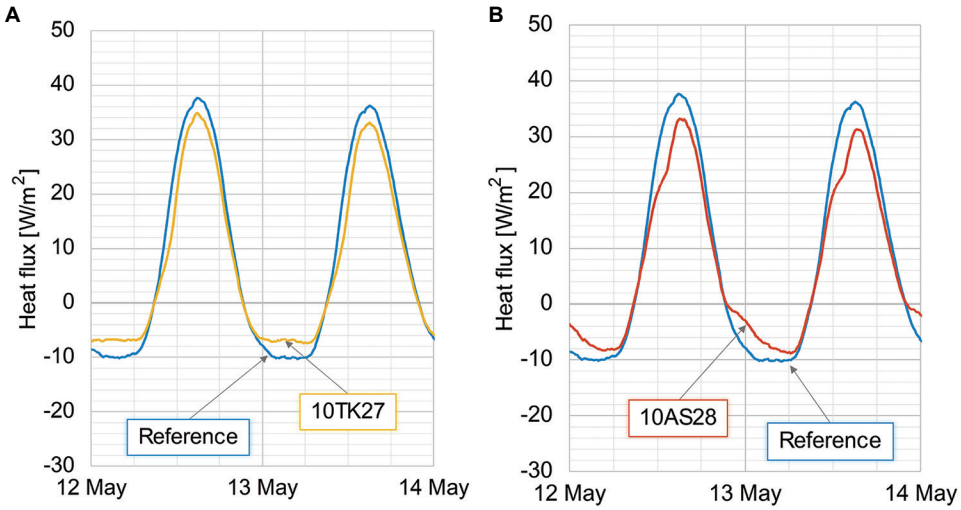

Figure 12. Comparison between heat fluxes of (A) 10TK27 and (B) 10AS28, compared to the reference, in period I

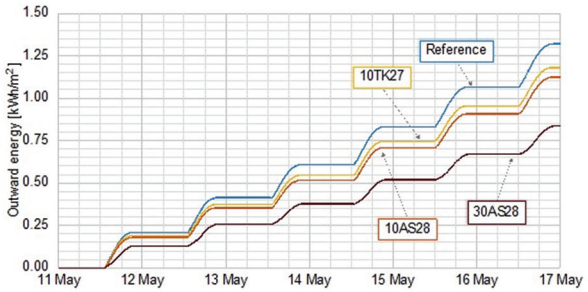

Figure 13. Outward energy for each of the wall samples in period I

the data acquired during the period I, the total energy transferred through each wall sample containing PCM was calculated and compared to that of the Reference. The analysis distinguished between the inward energy – primarily responsible for the energy demand for cooling (time interval 9:00 – 20:00) – and the outward energy (time interval 20:00 – 9:00). The calculated energy reductions were then correlated with boundary conditions, particularly the outdoor air temperature, to determine whether and at which temperatures the plasters containing PCM performed more effectively.

Reductions in the incoming energy compared to reference (100%) are depicted in Figure 15A. In the case of 10TK27, the energy difference is almost constant at every temperature; for 10AS28 and 30AS28 (with the same PCM), energy differences are more consistent in the temperature interval of 27 – 32°C, corresponding to the phase change interval of the PCM. Similar assumptions were made in Figure 15B regarding the outward energy during the night, where different PCM behaviors are notable. Minimum temperatures fluctuated between 7°C and 22°C; the greatest reduction in TK27 occurred at lower temperatures, while the lowest reduction was observed in AS28. The total incoming energy through the wall samples was calculated for the entire day (9:00 – 20:00) and the "critical" interval (12:00 – 15:00). In Table 3, the percentage differences between each wall sample containing PCM and the reference are reported, and there are notable improvements in all samples containing PCM. Considering the entire day, the energy reductions were 11.3% for 10TK27, 13.1% for 10AS28, and 35.1% for 30AS28. When considering only the critical interval, the reductions were 8.8% for 10TK27, 15.5% for 10AS28, and 49.7% for 30AS28. As for the outgoing energy, the reductions were 19.5%, 35.5%, and 87.5%, respectively. The greater reductions observed in the samples containing AS28 may be due to the higher phase-change temperature and narrower temperature interval compared to TK27.

3.2. Period II

The boundary conditions that characterized period II are reported in Table 4. A representative interval of 6 consecutive days (August 9 – 14, 2022) was selected. In terms of boundary conditions (Figure 16), the outdoor temperature fluctuated between 20°C and 35°C, with lower values on August 12 and 13. The solar irradiance values peaked between 750 W/m^2 and 850 W/m^2, with clear skies only on August 9 and 11. Temperatures on the outer plaster surfaces are depicted in Figure 17. In general, temperatures on the outer surfaces are relatively similar among the different wall samples, with differences slightly more prominent at night. Temperatures on the inner plaster surfaces are depicted in Figure 18. The fluctuation between minimum and maximum temperatures is limited and <6°C; hence, differences between the wall samples are minimal.

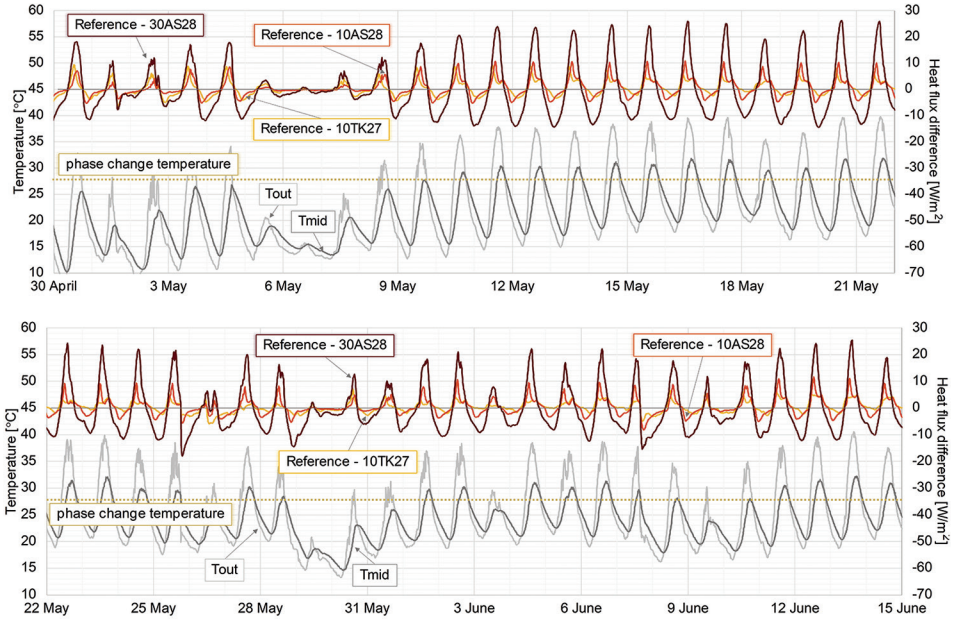

Figure 14. Comparison between heat fluxes in period I

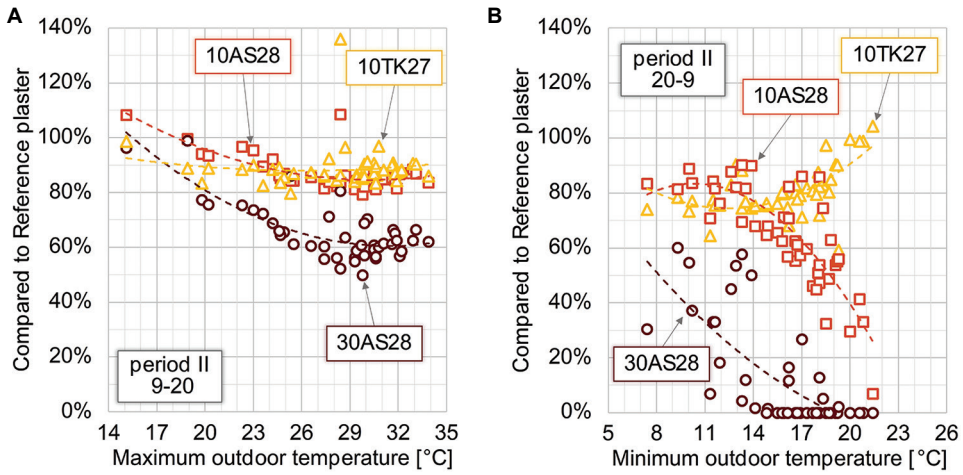

Figure 15. Energy reductions. (A) Reduction in inward energy compared to the reference according to the maximum outdoor temperature. (B) Reduction in outward energy compared to the reference according to the minimum outdoor temperature in period II.

Table 3. Percentage comparison of the energy through each wall sample compared to the reference in period I

Plaster	Energy difference compared to the reference (%)		
	Inward energy		Outward energy
	9:00 – 20:00	12:00 – 15:00	20:00 – 9:00
10TK27	−11.3	−8.8	−19.5
10AS28	−13.1	−15.5	−35.5
30AS28	−35.1	−49.7	−87.5

Temperatures on 10AS28 and 20AS28 are almost identical and differ from the Reference by <0.5°C; in the case of 30AS28, the maximum values are about 1°C lower, and the minimum values are about 1°C higher than the reference.

The temperature in the middle of the wall samples is depicted in Figure 19, and the temperature differences between the wall samples and the reference are depicted in Figure 20. In this case, the higher amount of PCM inside the plaster corresponded to an increase in the temperature difference monitored between the wall samples and the reference. During the day, 10% of PCM corresponded to a 1°C reduction, 20% of PCM to a 2 – 2.5°C reduction, and 30% of PCM to a 3 – 4°C reduction. During the night,

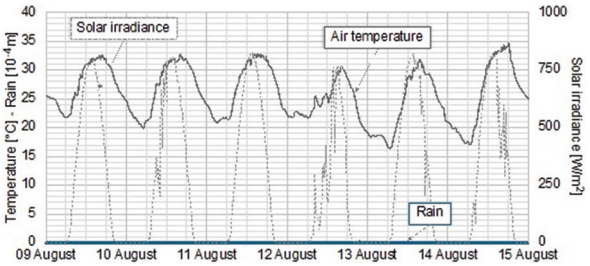

Figure 16. Boundary conditions in the selected interval in period II

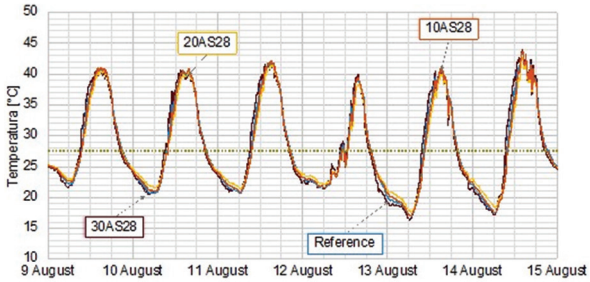

Figure 17. Outer surface temperatures (Tout) in period II

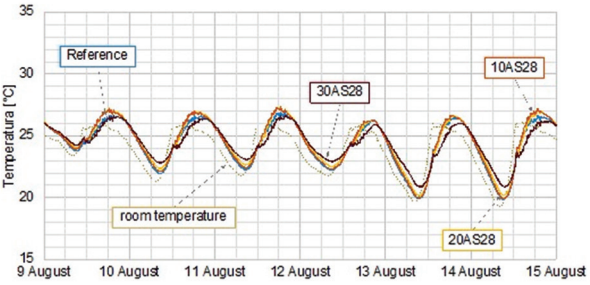

Figure 18. Inner surface temperatures (Tin) in period II

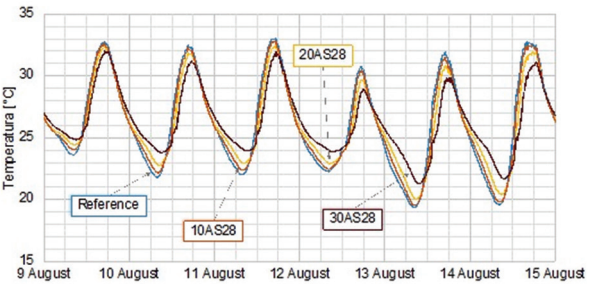

Figure 19. Temperatures in the middle (Tmid) of the wall samples in period II

the temperature of the Reference was the lowest, with differences of about 0.5°C with 10AS28, 1°C with 20AS28, and 2 – 3°C with 30AS28.

Monitored heat fluxes are depicted in Figure 21. During the day, the maximum values of reference, 10AS28, and 20AS28 were almost identical, while in 30AS28, the peaks

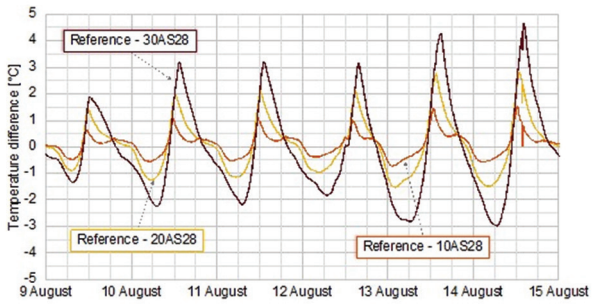

Figure 20. Temperature differences in the middle of the wall samples compared to the reference in period II

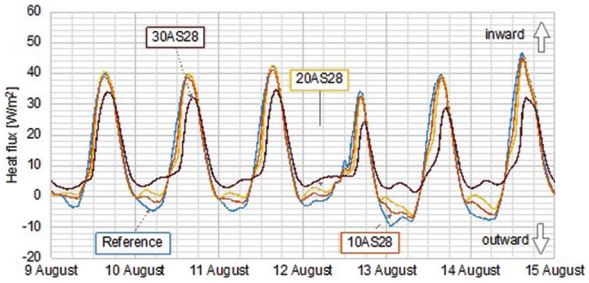

Figure 21. Heat fluxes in the middle of the wall samples

Table 4. Average boundary conditions in period II

Condition	Day	Night	Interval
Average outdoor temperature (°C)	29.3	22.6	30.5
Maximum outdoor temperature (°C)	39.6	30.7	38.7
Minimum outdoor temperature (°C)	17.4	16.4	19.8
Average indoor temperature (°C)	25.2	23.3	25.8
Average solar irradiance (W/m²)	433	24	662
Maximum solar irradiance (W/m²)	884	434	884
Solar gain (kWh/[m² day])	5.19	0.28	2.65

Note: The time intervals are defined as: (i) Day: 9:00 – 20:00; (ii) Night: 20:00 – 9:00; and (iii) Interval: 12:00 – 15:00.

were 6 – 8 W/m² lower. In all samples containing PCM, the phase change could be observed both during melting and solidification through changes in the curves' slope. The total inward energy through each wall sample was then calculated, taking into consideration the working period of the fan coil (Figure 22). The total inward energy was 1.63 kWh/m² for the reference, 1.50 kWh/m² for 10AS28, 1.46 kWh/m² for 20AS28, and 1.21 kWh/m² for 30AS28, corresponding to relative reductions (compared to the reference) of 7.9%, 10.4%, and 25.8%, respectively.

In Figure 23, the differences between the heat flux through the reference and that of each of the other wall samples are depicted alongside temperatures of the outer plaster surface of the reference and the middle of the wall.

In this case, the three curves, corresponding to plasters containing different quantities of the same PCM, displayed a similar trend, with proportional differences between the reference and PCM quantity. Based on all the data acquired during the period, the energy through each wall sample was calculated, differentiating between the inward (time interval 9:00 – 20:00) and the outward energy (20:00 – 9:00) and subsequently comparing them to the reference.

The energy reductions were then correlated to the outdoor temperature; Figure 24A and B depict the maximum and minimum temperatures, respectively. During the day, almost no difference could be observed between the various maximum temperatures, with average reductions of 8 – 10% for 10AS28, 12 – 15% for 20AS28, and 25 – 30% for 30AS28. During the night, the reduction was significantly different, as PCM solidification involves the partial release of the absorbed heat, leading to incoming heat fluxes – unlike the Reference, where night-time heat fluxes were consistently outward. The percentage differences with respect to the reference were calculated both during the day (9:00 – 20:00) and the critical interval (12:00 – 15:00) (Table 5). The reductions during the day were 7.6% for 10AS28, 10.6% for 20AS28, and 24.6% for 30AS28; the reductions in the critical interval were about 5.2% for 10AS28, 12.1% for 20AS28, and 39.2% for 30AS28. Similarly, the outgoing energy reductions were 91.8% for 10AS28, 91.6% for 20AS28, and 100% for 30AS28, which, as previously mentioned, were due to the incoming heat fluxes during the night. However, despite the promising results in terms of temperatures and heat flux for the plaster containing 30% PCM, a progressive deterioration of the plaster was observed during monitoring (Figure 7). This degradation was most likely due to the volumetric expansion of the PCM during the phase change, which was exacerbated by the high mass ratio of PCM inside the plaster. It was estimated that 30% by mass of PCM corresponded to approximately 44% by volume. Consequently, further developments of the research will focus only on plasters with 10% and 20% PCM by mass.

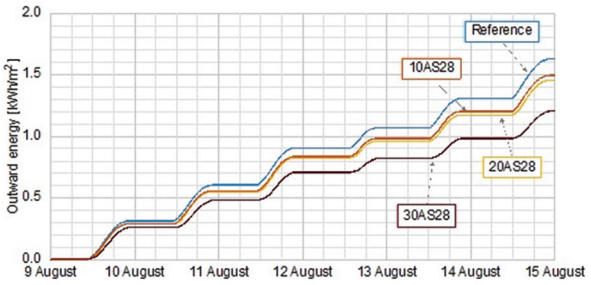

Figure 22. Inward energy for each of the wall samples

3.3. General considerations

In general, further considerations about the entire monitoring period were possible because the reference, 10AS28, and 30AS28 samples were kept unchanged throughout the monitoring. The percentage differences in the incoming energy through the two walls containing PCM with respect to the reference are sorted according to the maximum outdoor temperature reached in Figure 25. In both cases, major reductions were observed when the maximum outdoor temperatures fell within the phase change range of the PCM, namely, between 27°C and 33°C. In general, reductions were visible at almost all temperatures, except when temperatures dropped below 15°C – conditions under which no cooling was required.

The average reduction for plasters that were maintained throughout the entire monitoring period was calculated (Table 6). For 10AS28, the total incoming energy during the day (9:00 – 20:00), when the room temperature was

Table 5. Percentage comparison of the energy through each wall sample compared to the reference in period II

Plaster	Energy difference compared to the reference (%)		
	Inward energy		Outward energy
	9:00 – 20:00	12:00 – 15:00	20:00 – 9:00
10AS28	−7.6	−5.2	−91.8
20AS28	−10.6	−12.1	−91.6
30AS28	−24.6	−39.2	−100.0

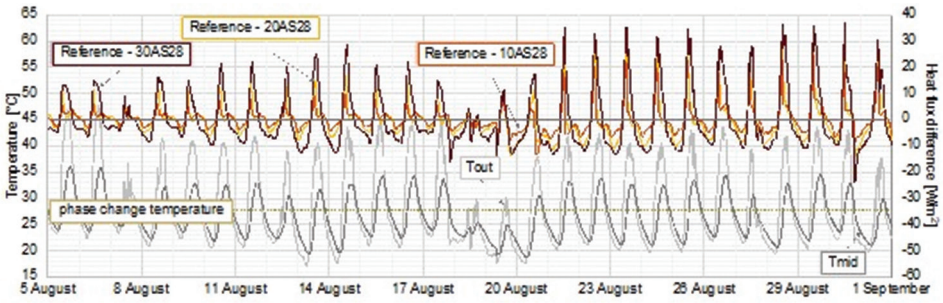

Figure 23. Comparison between heat fluxes in period II

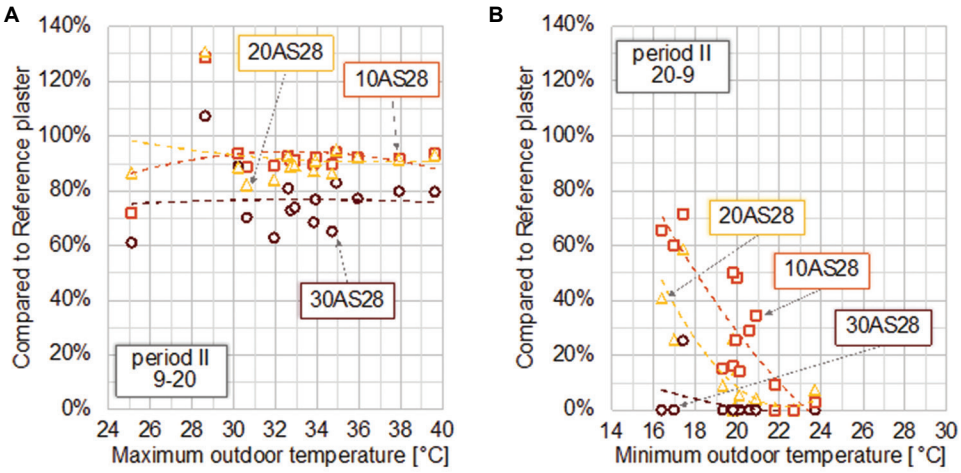

Figure 24. Energy reductions. (A) Reductions in inward energy compared to the Reference according to the maximum outdoor temperature. (B) Reduction in outward energy compared to the Reference according to the minimum outdoor temperature.

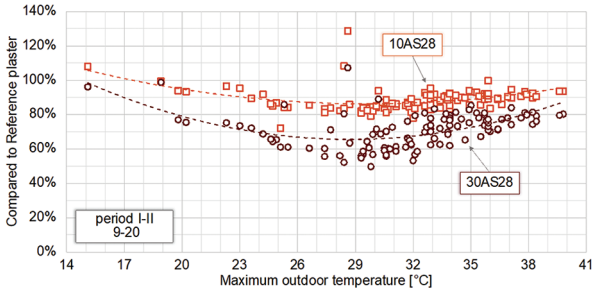

Figure 25. Reduction in inward energy compared to the reference, according to the maximum outdoor temperature in the entire monitoring period

Table 6. Percentage comparison of the energy through each wall sample compared to the reference in the entire monitoring period

Plaster	Energy difference compared to the reference (%)		
	Inward energy		Outward energy
	9:00 – 20:00	12:00 – 15:00	20:00 – 9:00
10AS28	−10.5	−9.9	−67.1
30AS28	−28.2	−42.0	−95.6

higher than 25°C, was 10.6% less than the reference; 12.6% when the temperature was lower than 25°C; and 9.9% at the critical interval (12:00 – 15:00). In terms of outdoor energy, the average reduction was 67.1%. In the case of 30AS28, the reductions were 28.4% and 29.0% when the room temperature was higher and lower than 25°C, respectively; 42% in the critical interval (12:00 – 15:00); and 95.6% in terms of outgoing energy. The consistent reductions that are visible during the night (outward heat flux) are probably due to PCM solidification, where part of the energy absorbed during the day is released inward.

4. Conclusion

The focus of this research was the development of plaster samples with different concentrations of PCM, which were then tested under real outdoor conditions for several weeks. Conducted in collaboration with Fassa Bortolo – an Italian industry leader in the production of mortars, pre-mixed plasters, paints, and thermal insulation. A dedicated setup was built to monitor up to four wall samples simultaneously, each of which was made of a thin masonry layer covered with plaster on both sides. One served as the reference sample, containing no PCM, while the others had exterior plasters containing different amounts of two different PCM.

Two relevant periods were considered. In the first period (period I), one of the wall samples was the reference sample (without PCM), while the other three wall samples contained PCM on the outer side, namely, 10TK27, 10AS28, and 30AS28. The results indicated that in both configurations with 10% PCM, the overall incoming energy was reduced by more than 10%; that is, 11.3% for 10TK27 and 13.1% for 10AS28. In the case of 30AS28, despite the weakening of the plaster, the reduction of the incoming energy reached about 35%. In the critical interval between 12:00 and 15:00, the reductions were 8.8% for 10TK27, 15.5% for 10AS28, and 49.7% for 30AS28. The difference between the two configurations containing 10% PCM could be attributed to the different melting ranges of the PCM; for example, 10TK27 completely melted before 12:00.

In the second period (period II), after having observed the degradation of 30AS28 due to an excessive amount of PCM, the configuration with 10TK27 was replaced with 20AS28 to simultaneously compare the effect of PCM

concentration within the plaster. During this period, the incorporation of 10% PCM by mass led to a reduction of nearly 8% in incoming energy during the day, while 20% and 30% PCM resulted in reductions of over 10% and nearly 25%, respectively. Between the critical interval (12:00 – 15:00), the reductions were 5.2%, 12.1%, and 39.2%, respectively. The lower reduction of 10% PCM was most likely due to the fact that the small amount of PCM had completely melted. However, in terms of temperatures and heat fluxes, only 10% and 20% PCM could be considered a feasible solution for the energy refurbishment of buildings, as plasters containing 30% PCM could suffer from excessive deterioration due to the volumetric expansion of the PCM between the solid and liquid states.

The positive outcome of this research should encourage further developments aimed at extending the results to the integration of PCM within the plaster across the entire building envelope. This next phase would enable the exploration of different aspects that were not considered in this study. In particular, it would allow for an assessment of the effect of building orientation. At a preliminary level, it is important to consider that different wall orientations can lead to varying wall surface temperatures, potentially resulting in conditions that fall outside the optimal PCM melting range. In such cases, the material may not be fully solidified and/or melted. In addition, even when a complete charging and discharging cycle of the PCM occurs, the transition timing may vary depending on orientation; if the wall is east-oriented, the phase change may occur earlier than in a south-oriented wall; if the wall is west-oriented, the phase change may occur later than in a south-oriented wall. While this would not affect the latent heat capacity of the PCM, it does influence the specific period in which the PCM phase change occurs. Second, an extension of these results could lead to the exploration of different climatic contexts to assess whether the behavior observed with the climate of Ferrara (Köppen Geiger zone Cfa) remains consistent in other climate zones. Third, an application at the building scale would allow the evaluation of indoor thermal comfort and the effect of the PCM. At the scale of the present study, such considerations were not possible given the size of the samples and the application on a mock-up building, typically used for experimental research purposes. An experimental upgrade of this research, involving full-scale building applications, could confirm the preliminary findings (i.e., the addition of PCM does not lead to any additional problems) or reveal aspects not yet considered in the present research.

Acknowledgments

The results presented here were part of a wider research that is being conducted with the financial support of Fassa Bortolo,[15] whose contribution is gratefully acknowledged for enabling the publication of these findings.

Funding

This research was carried out with the financial support of Fassa Bortolo, an Italian industry leader in the production of pre-mixed plasters and mortars.

Conflict of interest

Michele Bottarelli is an Editorial Board Member of this journal but was not in any way involved in the editorial and peer-review process conducted for this paper, directly or indirectly. Separately, Eleonora Baccega declared that having no known competing financial interests or personal relationships could have influenced the work reported in this paper.

Author contributions

Conceptualization: All authors
Formal analysis: Eleonora Baccega
Investigation: Eleonora Baccega
Methodology: All authors
Supervision: Michele Bottarelli
Validation: Michele Bottarelli
Writing – original draft: Eleonora Baccega
Writing – review & editing: All authors

Ethics approval and consent to participate

Not applicable.

Consent for publication

Not applicable.

Availability of data

Data obtained in this study may be made available upon reasonable request from the corresponding author after obtaining authorization from the funding company.

Further disclosure

Part of or the entire set of findings has been presented in a conference (SET2024 Shanghai, 2024).

References

1. Sinka M, Bajare D, Jakovics A, Ratnieks J, Gendelis S, Tihana J. Experimental testing of phase change materials in a warm-summer humid continental climate. *Energy Build.* 2019;195:205-215.

   doi: 10.1016/j.enbuild.2019.04.030

2. Asadi E, da Silva MG, Antunes CH, Dias L. Multi-objective optimization for building retrofit strategies: A model and an

application. *Energy Build.* 2012;44:81-87.

doi: 10.1016/j.enbuild.2011.10.016

3. *Global Status Report for Buildings and Construction*. Available from: https://globalabc.org/resources/publications/2020-global-status-report-buildings-and-construction [Last accessed on 2022 Mar 15].
4. Pandey B, Banerjee R, Sharma A. Coupled EnergyPlus and CFD analysis of PCM for thermal management of buildings. *Energy Build.* 2021;231:110598.

   doi: 10.1016/j.enbuild.2020.110598
5. Pavlik Z, Trnik A, Keppert M, Pavlikova M, Zumar J, Cerny R. Experimental investigation of the properties of lime-based plaster-containing PCM for enhancing the heat-storage capacity of building envelope. *Int J Thermophys*. 2014;195:205-215.

   doi: 10.1007/s10765-013-1550-8
6. Coppola L, Coffetti D, Lorenzi S. Cement-based renders manufactured with phase-change materials: Applications and feasibility. *Adv Mater Sci Eng*. 2016;2016:7254823.

   doi: 10.1155/2016/7254823
7. Milone D, Peri G, Pitruzzella S, Rizzo G. Are the best available technologies the only viable for energy interventions in historical buildings? *Energy Build.* 2015;95:39-46.

   doi: 10.1016/j.enbuild.2014.11.004
8. *European Parliament, Boosting Building Renovation: What Potential and Value for Europe?* Available from: https://www.europarl.europa.eu/regdata/etudes/stud/2016/587326/ipol_stu(2016)587326_en.pdf [Last accessed on 2022 Mar 17].
9. Pajek L, Potočnik J, Košir M. The effect of a warming climate on the relevance of passive design measures for heating and cooling of European single-family detached buildings. *Energy Build.* 2022;251:111947.

   doi: 10.1016/j.enbuild.2022.111947
10. Song Y, Darani KS, Khdair AI, Abu-Rumman G, Kalbasi R. A review on conventional passive cooling methods applicable to arid and warm climates considering economic cost and efficiency analysis in resource-based cities. *Energy Rep.* 2021;7:2784-2820.

    doi: 10.1016/j.egyr.2021.04.056
11. Akeiber H, Nejat P, Majid MZA, *et al.* A review on phase change material (PCM) for sustainable passive cooling in building envelopes. *Renew Sustain Energy Rev.* 2016;60:1470-1497.

    doi: 10.1016/j.rser.2016.03.036
12. Sá AV, Azenha M, de Sousa H, Samagaio A. Thermal enhancement of plastering mortars with phase change materials: Experimental and numerical approach. *Energy Build.* 2012;49:16-27.

    doi: 10.1016/j.enbuild.2012.02.031
13. Baccega E, Bottarelli M, Su Y. Alternative experimental characterization of phase change material plasterboard using two-step temperature ramping technique. *Energy Build.* 2022;267:112153.

    doi: 10.1016/j.enbuild.2022.112153
14. Baccega E. Thermo-physical characterisation of plasters containing phase change materials (PCMs). *Int J Thermophys*. 2024;45:33.

    doi: 10.1007/s10765-023-03327-7
15. Fassa S. Available from: https://www.fassabortolo.it/it [Last accessed on 2022 Jan 22].
16. *HEROTILE - High Energy Savings in Building Cooling by Roof Tiles Shape Optimization toward a Better above Sheathing Ventilation*. Available from: https://www.lifeherotile.eu/it [Last accessed on 2021 Jan 12].
17. Hukseflux FHF04. Available from: https://www.hukseflux.com/products/heat-flux-sensors/heat-flux-sensors/fhf04-heat-flux-sensor [Last accessed on 2023 Jan 13].
18. DataTaker. Available from: https://www.thermofisher.com/order/catalog/product/DT85?SID=srch-srp-DT85 [Last accessed on 2023 Jan 13].
19. Davis Vantage Pro2. Available from: https://www.davisinstruments.com/pages/vantage-pro2 [Last accessed on 2023 Jan 13].
20. Hukseflux SR20. Available from: https://www.hukseflux.com/products/pyranometers-solar-radiation-sensors/pyranometers/sr20-pyranometer [Last accessed on 2023 Jan 13].
21. Smart Advanced Systems GmbH. Available from: https://www.smart-advanced-systems.de [Last accessed on 2023 Jul 01].
22. *TITK- Thüringisches Institut für Textil- und Kunststoff-Forschung*. Available from: https://www.titk.de [Last accessed on 2021 Dec 01].